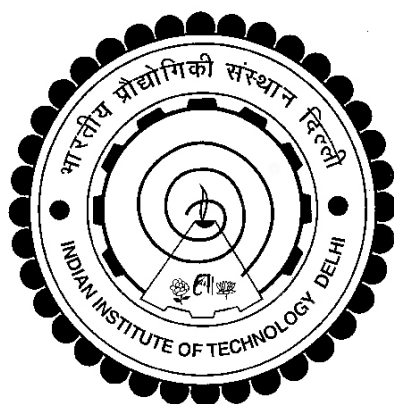


STUDIES ON POLYLACTIDE BASED BLENDS AND NANOCOMPOSITES

RANJANA NEHRA



**DEPARTMENT OF MATERIAL SCIENCE AND ENGINEERING
INDIAN INSTITUTE OF TECHNOLOGY DELHI**

MAY 2018

©Indian Institute of Technology Delhi (IITD), New Delhi, 2018

STUDIES ON POLYLACTIDE BASED BLENDS AND NANOCOMPOSITES

by

RANJANA NEHRA

Department of Material Science and Engineering

Submitted

In fulfilment of the requirements of the degree of Doctor of Philosophy

to the



INDIAN INSTITUTE OF TECHNOLOGY DELHI

MAY 2018

CERTIFICATE

This is to certify that the thesis entitled “**Studies on polylactide based blends and nanocomposites**” being submitted by **Ms. Ranjana Nehra**, to the Indian Institute of Technology Delhi, for the award of the degree of **Doctor of Philosophy** in the Department of Material Science and Engineering, is a record of bonafide research work carried out by her. This thesis has been prepared in conformity with the rules and regulations of the Indian Institute of Technology Delhi, New Delhi. The thesis, in our opinion, is worthy of consideration for award of the degree of Doctor of Philosophy in accordance with the regulations of the Institute.

The results contained in this thesis have not been submitted, in part or full, to any other university or Institute for the award of any degree or diploma.

Dr Saurindra Nath Maiti

Emeritus Professor

Department of Material Science and Engineering
Indian Institute of Technology Delhi
New Delhi-110016, India

Dr Josemon Jacob

Professor

Department of Material Science and Engineering
Indian Institute of Technology Delhi
New Delhi-110016, India

Acknowledgements

With deep sense of gratitude and sincere regards, I would like to acknowledge the guidance and encouragement given by my supervisors, Prof. S. N. Maiti and Prof. Josemon Jacob for this research work. The inspirational and insightful discussion with Prof. Maiti imbibed the spirit in me which always kept me going by focusing in my job.

I express my sincere thanks to my SRC members, Prof. Anup K. Ghosh, Dr. Bhabhani K. Satapathy and Prof. Manjeet Jassal for their constructive criticism and valuable suggestions. My special appreciation to Prof. Veena Choudhary, Prof. Harpal Singh, Dr Leena Nebhani, Dr Sampa Saha and Dr Bijay P Tripathi for their goodwill and support for my study here at DMSE, IIT Delhi.

I feel immense honour and pride to acknowledge Indian Institute of Technology Delhi, for providing me excellent environment and facilities throughout my study period. I convey my deep regards and thanks to the Council of Scientific & Industrial Research (CSIR), New Delhi, India (file no. 09/086(1034)/2010-EMR-I) and Ministry of Human Resource Development (MHRD), Government of India, for providing me research funding for my PhD degree at IIT Delhi.

In regards to the testing of materials, I thank Mr. Surinder Sharma and Mr. Ashok Kapoor of DMSE for their cooperation while sample testing. I am thankful to the staff members Mr. Shiv Kant, Mr. Ehteshamaul Islam and Mr. Gajraj Singh for extending a helping hand whenever needed. I am grateful to Mr. D. C. Sharma and Mr. Kuldeep Sharma of SEM central facility for teaching and allowing me to do scan of samples using the SEM instrument. Also, I thank Department of Physics and Department of Textile for providing me the facilities to carry out the XRD and FESEM testing, respectively. I would also like to convey my thanks to Shalini Arora, Sudhir Kumar Pandey and Pramod Kale for their all possible supports.

I am indebted to my dear friends Dr Achla Tripathi, Dr Rajendra Singla, Dr Astha Garhwal, Sabhapati Sankarpandi, Sampat Singh Chauhan, Dr Tahir Zafar, Dr Pawan Verma, Viswa Pratap Singh, Dr Bindu Manchanda, who are incredibly talented and resourceful that helped me a lot during the course of experiment as well as while analyzing the raw data. I also thank Prajesh Nayak, Smrutirekha Mishra for their kind cooperation. My friends Shilpi Sharma, Savita Meena, Ritima Banerjee, Debanga B. Konwar, Bhavna Sharma, Banpreet Kaur, Dr Manisha Tomar, Dr Richkant, Kanika Modi, Dr Manchal Choudhary, Dr

Sapna Mishra, Dr Aashima Malik are greatly thanked for being an incredible support system and their encouraging words throughout my PhD.

I am thankful to all my friends and colleagues, Dr Hemlata, Dr Rishi Sharma, Dr Rajul Sharma, Dr Abhishek Gandhi, Dr Harjeet Singh Jaggi, Dr Sanjeev Kumar, Dr Jutika Goswami, Dr Sneh Bharti, Dr Shikha Jain, Agni Kr. Biswal, Shikha, Dr Priyanka Singh, Rakesh Kachhap, Deepika Malpani, Reshu Tyagi, Anindya Dutta, Pragati Gahlout, Devendra Kumar, Sumbul Hafeez, Harshita, Bariya Qayyum, Neetu Kumari, Srijita Purkayastha, Shubhra Goel, Kalpana Pandey, Sucharita Sethy, Ifra, for providing a congenial and super-friendly environment to work with. I am grateful to the office bearers as well for their kind cooperation in official matters.

I also share the credit of my work with my loving husband, Dr Jagdish Prasad who has been continuously acting as my energy house in shaping my career. He is a person who never lets negativity to come in. My little son (Darshil Sigar) has been the relaxant for me during those stressful moments and I owe a lot to him. I thank other family members of my in-laws who have always been loving and caring to me.

I owe my deepest gratitude to my sisters Savita Nehra and Mamta Nehra without whom I would not have complete my PhD. I especially thanks my parents Raghunath Prasad Nehra and Mohini Nehra who have taught me to be hard working and devoted in life, whatever I do and they both have been great encouragement to me. My sisters Dr Anita Nehra, Rashmi Nehra and brothers Ram Krishna Rohit, Ravi Shankar Ankur have always supported me with their unconditional love and care, and my deep regards are always with them who have been with me when times are rough.

Finally, I thank the 'ALMIGHTY GOD' for his blessings and further seek him to provide me blessings, patience and strength to accomplish newer goals.

Date

Ranjana Nehra

Place: New Delhi

ABSTRACT

Biobased polymers have received a great deal of attention because of their superior eco-friendliness and advantages to minimize the usage of petrochemical resources. Polylactide (PLA) is a biodegradable, linear aliphatic thermoplastic polyester which is derived from renewable plant origins. PLA possesses good transparency, high tensile strength and modulus making it a possible alternative for petroleum-based plastics such as poly(ethylene terephthalate), polystyrene and polypropylene. However, due to its brittleness, difficult processability, low thermal stability and toughness, neat PLA finds limited applications.

In order to toughen PLA mainly plasticization, blending and copolymerization methods are used. PLA was melt mixed with poly(ethylene glycol) (PEG) with molecular weight of 4000 g/mol in various PEG concentrations (5-30 wt%). Tensile strength and modulus of PLA decreased in a linear fashion with increasing PEG content. PEG improved the flexibility and plastic deformation of PLA by reducing the intermolecular forces. The impact strength remained almost constant at low PEG content and enhanced significantly at maximum PEG concentration. However, PEG improved the impact strength properties at the cost of tensile strength. Differential scanning calorimetry (DSC) showed PEG incorporation reduced the T_g of PLA significantly. The melt crystallinity of PLA enhanced with increase in PEG content. The effect of PEG incorporation on thermal stability of PLA was characterised by thermo gravimetric analysis (TGA). Thermomechanical behaviour of the blends was studied by dynamic mechanical analysis (DMA). The shear viscosity of PLA decreased significantly with increase in PEG content.

Blending with a thermoplastic elastomer like poly(styrene-*b*-ethylene-*co*-butylene-*b*-styrene)-*g*-maleic anhydride copolymer (SEBS-*g*-MA) can be an effective way to toughen PLA. SEBS-*g*-MA improves impact strength and flexibility of brittle polymers with minimum decrease in stiffness. PLA was melt blended with SEBS-*g*-MA copolymer in varied

concentration (5-40 wt%). The blends thus prepared, were characterized by various test methods such as mechanical (tensile and impact), thermal (TGA, DSC), thermomechanical, rheological (capillary and parallel plate rheometry), morphological and fracture analyses. SEBS-g-MA incorporation enhanced elongation-at-break and Izod impact strength with minimum decrease in tensile strength and modulus. Theoretical models were employed to analyze the tensile properties of the blends in order to evaluate the blend structure. The microstructural attributes were characterized by scanning electron microscopy (SEM) of cryofractured, impact fractured and tensile fractured surfaces.

Sepiolite nanoclay is used as reinforcing agent for PLA/SEBS-g-MA 90/10 (w/w) blend. Effects of sepiolite on thermal behaviour, morphology and thermo-mechanical properties of PLA/SEBS-g-MA blend were investigated. The nanocomposite exhibited increase in the tensile modulus and toughness as compared to the blend matrix. Tensile strength and impact strength properties were almost unaffected with sepiolite incorporation. Field emission scanning electron microscopy and transmission electron microscopy images exhibited sepiolite induced morphological changes and dispersion of sepiolite in both PLA and SEBS-g-MA phases. DMA and wide angle X-ray diffraction presented evidences in support of the reinforcing nature of sepiolite and phase interaction between the filler and the matrix.

In future, PLA/SEBS-g-MA/sepiolite ternary nanocomposites can be explored for applications in services e.g. wares, folded cartons, durable goods, laptop and mobile housing, packaging and automotives. PLA/PEG blends can be inducted to nondurable applications in short term molded applications.

सार

जैव आधारित पॉलिमर को पेट्रोकेमिकल संसाधनों के उपयोग को कम करने के लिए उनके श्रेष्ठ पर्यावरण-मित्रता और फायदों के कारण बहुत ध्यान दिया गया है। पोलिलाक्टाइड (पीएलए) एक बायोडिग्रेडेबल, रैखिक एलिफैटिक थर्मोप्लास्टिक पॉलिएस्टर है जो नवीकरणीय पौधे की उत्पत्ति से लिया गया है। पीएलए में अच्छी पारदर्शिता, उच्च तन्यता ताकत और मॉड्यूलस है जो इसे पॉली (एथिलीन टेरैफेथलेट), पॉलीस्टाइरिन और पॉलीप्रोपाइलीन जैसे पेट्रोलियम-आधारित प्लास्टिक के लिए एक संभावित विकल्प बनाता है। हालांकि, इसकी कठिन प्रक्रियाशीलता, कम थर्मल स्थिरता, कठोरता और भंगुरता के कारण, साफ पीएलए सीमित अनुप्रयोगों को पाता है।

पीएलए को सख्त करने के लिए मुख्य रूप से प्लास्टाइजेशन, मिश्रण और कोपोलिमेराइजेशन विधियों का उपयोग किया जाता है। पीएलए को विभिन्न पॉली (एथिलीन ग्लाइकोल) (पीईजी) सांद्रता (5-30 वजन%) में 4000 ग्राम/मोल के आणविक वजन के साथ पीईजी के साथ मिश्रित पिघल गया था। पीएलए की तन्यता ताकत और मॉड्यूलस पीईजी वजन% बढ़ने के साथ एक रैखिक फैशन में कमी आई है। पीईजी ने आणविक बलों को कम करके पीएलए की लचीलापन और प्लास्टिक विरूपण में सुधार किया। कम पीईजी भार पर प्रभाव शक्ति लगभग स्थिर रही और अधिकतम पीईजी भार पर उल्लेखनीय रूप से वृद्धि हुई। हालांकि, पीईजी तन्य शक्ति की लागत पर प्रभाव शक्ति गुणों में सुधार हुआ। अंतरकारी स्कैनिंग कैलोरीमेट्री (डीएससी) ने दिखाया कि पीईजी समावेश ने पीएलए के टीजी को काफी कम कर दिया है। पीएलए की पिघलने वाली क्रिस्टलीयता पीईजी भार में वृद्धि के साथ बढ़ी है। पीएलए की थर्मल स्थिरता पर पीईजी समावेश का प्रभाव थर्मो ग्रेविमेट्रिक विश्लेषण (टीजीए) द्वारा वर्णन किया गया था। मिश्रणों के थर्मोमेकेनिकल व्यवहार का अध्ययन गतिशील यांत्रिक विश्लेषण (डीएमए) द्वारा किया गया था। पीएलए की अपरूपण श्यानता में पीईजी भार में वृद्धि के साथ उल्लेखनीय रूप से कमी आई है।

पीएलए को सख्त करने एक प्रभावी तरीका पॉली(स्टायरिन-ब्लॉक-एथिलीन-सह-ब्यूटिलीन-ब्लॉक-स्टायरिन)-ग्राफ्टेड-मैलेइकएनहाइड्राइड कोपोलिमर (एसईबीएस-जी-एमए) जैसे थर्मोप्लास्टिक इलास्टोमर के साथ मिश्रण हो सकता है। एसईबीएस-जी-एमए भंगुर बहुलकों की कठोरता में न्यूनतम कमी के साथ इम्पैक्ट ताकत और लचीलापन में सुधार करता है। विभिन्न सांद्रता (5-40 वजन%) में एसईबीएस-जी-एमए कोपोलिमर के साथ पीएलए मिश्रित पिघलाया गया था। इस प्रकार तैयार किए गए मिश्रणों को यांत्रिक (तन्यता और इम्पैक्ट), थर्मल (टीजीए, डीएससी), थर्मोमेकेनिकल, रियोलॉजिकल (केशिका और समांतर प्लेट रियोमेट्री), मॉर्फोलॉजिकल और फ्रैक्चर विश्लेषण जैसे विभिन्न परीक्षण विधियों द्वारा निरूपण किया गया था। एसईबीएस-जी-एमए निगमन में तन्यता शक्ति और मॉड्यूलस में

न्यूनतम कमी के साथ बढ़ी हुई लम्बाई और आइजोड इम्पैक्ट शक्ति बढ़ी। सैद्धांतिक मॉडल मिश्रणों के तन्य गुणों का विश्लेषण करने के लिए नियोजित किए गए थे ताकि मिश्रण संरचना का मूल्यांकन किया जा सके। सूक्ष्म संरचनात्मक गुणों को क्रायफ्रैक्चरर्ड, इम्पैक्ट फ्रैक्चरर्ड और तन्यता फ्रैक्चर सतहों के इलेक्ट्रॉन माइक्रोस्कोपी (एसईएम) से स्कैन करके जांच किए गए थे।

सेपियोलाइट नैनोकले पीएलए/एसईबीएस-जी-एमए 90/10 (भार/भार) मिश्रण के लिए प्रबल करने वाले एजेंट के रूप में प्रयोग किया जाता है। थर्मल व्यवहार, मोर्फोलॉजी और पीएलए/एसईबीएस-जी-एमए मिश्रण के थर्मो-मैकेनिकल गुणों पर सेपियोलाइट के प्रभाव की जांच की गई। मिश्रण मैट्रिक्स की तुलना में नैनोकंपोजिट्स ने तन्यता मॉड्यूलस और कठोरता में वृद्धि देखी। तन्यता शक्ति और प्रभाव शक्ति गुण सेपियोलाइट निगमन के साथ लगभग अप्रभावित थे। फील्ड उत्सर्जन स्कैनिंग इलेक्ट्रॉन माइक्रोस्कोपी और ट्रांसमिशन इलेक्ट्रॉन माइक्रोस्कोपी छवियों ने पीएलए और एसईबीएस-जी-एमए अवस्थाओं में सेपियोलाइट प्रेरित मोर्फोलॉजिकल परिवर्तन और सेपियोलाइट का फैलाव प्रदर्शित किया। डीएमए और चौड़े कोण एक्स-रे विवर्तन ने सेपियोलाइट की सुदृढ़ बनाने की प्रकृति और फिलर और मैट्रिक्स के बीच अवस्थाओं के परस्पर क्रिया के समर्थन में साक्ष्य प्रस्तुत किए।

भविष्य में, पीएलए/एसईबीएस-जी-एमए/सेपियोलाइट टर्नरी नैनोकंपोजिट्स का उपयोग सेवाओं में अनुप्रयोगों के लिए लिया जा सकता है, जैसे की फोल्ड किए गए डिब्बे, टिकाऊ सामान, लैपटॉप और मोबाइल हाउसिंग, पैकेजिंग और ऑटोमोटिव इत्यादि। पीएलए/पीईजी मिश्रणों को अल्पकालिक मोल्डेड अनुप्रयोगों में काम में लिया जा सकता है।

Table of contents

Acknowledgements	i
Abstract	iii
List of contents	v
List of figures	ix
List of table	xiv
List of abbreviations	xvi
Chapter 1. Introduction and literature survey	1-45
1.1 Introduction	1
1.2 Biodegradable polymers	1
1.2.1 Categories of biodegradable polymers	2
1.2.2 Applications of biodegradable polymers	2
1.3 PLA	3
1.3.1 Synthesis of PLA	3
1.3.2 Properties of PLA	6
1.3.3 Advantages of PLA	12
1.3.4 Limitations of PLA	12
1.3.5 Applications of PLA	13
1.3.6 PLA toughening methods	13
1.4 PEG	16
1.4.1 Literature survey for PLA/PEG blend	16
1.5 Blends of PLA	18
1.5.1 SEBS-g-MA: a thermoplastic elastomer	21
1.5.2 SEBS-g-MA as impact modifier in different polymers	22
1.5.3 PLA/SEBS-g-MA blends	23
1.6 Nanocomposites	23
1.6.1 Classification of clays	24
1.6.2 Polymer layered silicate nanocomposites	25
1.7 Sepiolite	28
1.7.1 Sepiolite based nanocomposites	29
1.7.2 PLA/sepiolite nanocomposites	31
1.8 PLA based blend matrix nanocomposites	31

1.9	Summary of literature	33
1.10	Gaps in literature	34
1.10	Objective of the present work	34
1.11.	References	36
Chapter 2: Materials and methods		46-57
2.1	Overview of the chapter	46
2.2	Raw materials	46
2.3	Compositions and sample preparation	46
	2.3.1 PLA/PEG blends	46
	2.3.2 PLA/SEBS-g-MA blends and PLA/SEBS-g-MA/sepiolite nanocomposites	48
	2.3.2.1 Composition of blends and nanocomposites	48
	2.3.2.2 Melt blending via micro compounder	49
	2.3.2.3 Melt blending via twin screw extruder	49
2.4	Characterization and evaluation techniques	50
	2.4.1 Thermal characterization	50
	2.4.1.1 DSC study	50
	2.4.1.2 TGA	51
	2.4.2 Mechanical properties	51
	2.4.2.1 Tensile test	51
	2.4.2.2 Impact properties	52
	2.4.2.3 Flexural properties	52
	2.4.3 Morphological characterization	52
	2.4.3.1 Scanning electron microscopy (SEM)	52
	2.4.3.2 Field emission scanning electron microscopy (FESEM)	53
	2.4.3.3 Transmission electron microscopy (TEM)	53
	2.4.4 Dynamic mechanical analysis (DMA)	54
	2.4.5 Rheological characterization	54
	2.4.5.1 Parallel plate rheology	54
	2.4.5.2 Capillary rheology	54
	2.4.6 Wide angle X-ray diffraction (WAXD)	55
	2.4.7 Fracture analysis	55
	2.4.7.1 Essential work of fracture (EWF) concept	55
	2.4.7.2 EWF measurements	56
2.5	References	57

Chapter 3: Comparison of toughening of PLA by PEG and SEBS-g-MA	58-70
3.1 Overview of the chapter	58
3.2 PLA/PEG blends	58
3.2.1 Tensile properties	58
3.2.2 Impact strength	62
3.3 PLA/SEBS-g-MA blends	63
3.3.1 Tensile properties	63
3.3.1.1 Tensile Strength	64
3.3.1.2 Tensile Modulus	64
3.3.1.3 Elongation-at-break	66
3.3.2 Impact properties	66
3.4 Conclusions	67
3.5 References	70
Chapter 4: Studies on dynamic mechanical, thermal, rheological and fracture behaviour of PLA/SEBS-g-MA blends	71-106
4.1 Overview of the chapter	71
4.2 DMA	71
4.3 DSC studies	74
4.4 TGA	76
4.5 Predictive models for the tensile properties	78
4.5.1 Tensile Strength	78
4.5.2 Tensile Modulus	81
4.5.3 Elongation-at-break	82
4.6 SEM observations	83
4.7 WAXD study	87
4.8 Rheological properties	88
4.8.1 Parallel plate rheometry	88
4.8.2 Capillary rheometry	95
4.9 Fracture behaviour of the blends	96
4.10 Conclusions	101
4.11 References	104
Chapter 5: Thermal, mechanical and viscoelastic properties of PLA/SEBS-g-MA/sepiolite nanocomposites	107-134

5.1	Overview of the chapter	107
5.2	DSC studies	107
5.3	TGA studies	109
5.4	Mechanical properties	112
5.5	DMA studies	115
5.6	WAXD study	119
5.7	Morphological analysis	120
	5.7.1 Morphology of Cryofractured surfaces	120
	5.7.2 Morphology of impact fractured surfaces	122
	5.7.3 Morphology of tensile fractured surfaces	123
5.8	TEM observations	124
5.9	Dynamic oscillatory rheological analysis	125
5.10	Conclusions	131
5.11	References	133
Chapter 6: Thermal, dynamic mechanical and rheological properties of PLA/PEG blends		135-150
6.1.	Overview of the chapter	135
6.2	DSC analysis	135
6.3	DMA	138
6.4	TGA	141
6.5	Flexural properties	143
6.6	SEM	145
6.7	WAXD	146
6.8	Capillary rheometry	147
6.9	Conclusions	149
6.10	References	150
Chapter 7: Summary, conclusions and future scope		151-154
7.1	Summary of thesis	151
7.2	Conclusions	153
7.3	Probable applications of blends and nanocomposites	153
7.4	Recommendations for future study	154

List of Publications

Bio-data of the author

List of figures

Figure No.	Figure caption	Page No.
Chapter 1		
Figure 1.1	Optically active forms of lactic acid.	4
Figure 1.2	Synthesis route of PLA, from reference.	5
Figure 1.3	Petrochemical route of the production of PLA.	6
Figure 1.4	Comparison of the T_g and T_m of PLA with other thermoplastics [15].	7
Figure 1.5	Different forms of PLA obtained from the polymerization of various optically active configurations of lactic acid: (a) PLLA, (b) PDLA and (c) PDLLA.	9
Figure 1.6	Chemical structure of PEG.	16
Figure 1.7	Classification of clays based on their crystallographic pattern.	25
Figure 1.8	Schematic representation of different type of morphology arising from the interaction of layered silicates and polymers: (a) non-intercalated microcomposite (b) intercalated nanocomposites and (c) exfoliated nanocomposites.	26
Figure 1.9	Structure of sepiolite nanoclay.	29
Figure 1.10	Industrial applications of sepiolite.	30
Chapter 2		
Figure 2.1	A typical DENT specimen	57
Chapter 3		
Figure 3.1	Stress-strain curves for PLA and PLA/PEG blends.	59
Figure 3.2	Maximum stress vs. composition plots for PLA and PLA/PEG blends.	60
Figure 3.3	Tensile modulus curves for PLA and PLA/PEG blends.	61
Figure 3.4	Elongation-at-break curves for PLA and PLA/PEG blends.	61
Figure 3.5	Impact strength curves for PLA and PLA/PEG blends.	62
Figure 3.6	Variation of stress and strain with Φ_d in PLA/SEBS-g-MA blends. Inset: Variation of stress-strain for SEBS-g-MA.	63
Figure 3.7	Plots of tensile strength of PLA/SEBS-g-MA blends with Φ_d .	65
Figure 3.8	Plots of tensile modulus of PLA/SEBS-g-MA blends with Φ_d .	65
Figure 3.9	Plots of elongation-at-break of PLA/SEBS-g-MA blends with Φ_d .	66
Figure 3.10	Plots of impact strength of PLA/SEBS-g-MA blends with Φ_d .	67

Figure 3.11 Plots of tensile strength and impact strength vs. PLA/PEG blend compositions. 68

Figure 3.12 Plots of tensile strength and impact strength of PLA/SEBS-g-MA blends with Φ_d . 69

Chapter 4

Figure 4.1 Storage modulus curves of PLA, SEBS-g-MA and PLA/SEBS-g-MA blends. 72

Figure 4.2 Loss modulus curves of PLA, SEBS-g-MA and PLA/SEBS-g-MA blends. Inset: Expanded region from 45-80°C. 72

Figure 4.3 Tan δ curves of PLA, SEBS-g-MA and PLA/SEBS-g-MA blends. 73

Figure 4.4 DSC thermograms of PLA and PLA/SEBS-g-MA blend at 5°C/min. 75

Figure 4.5 TGA and d-TGA curves for PLA, SEBS-g-MA and PLA/SEBS-g-MA blends. 77

Figure 4.6 Plot of correlation of relative tensile strength with theoretical models. 79

Figure 4.7 Plot of correlation of relative tensile modulus with theoretical models. 81

Figure 4.8 Plot of correlation of relative elongation-at-break with Mitsubishi model. 82

Figure 4.9 Scanning electron micrographs of cryofractured samples of PLA/SEBS-g-MA blends at varying Φ_d : (a) 0, (b) 0.07 and its magnified image as inset, (c) 0.13 and its magnified image as inset, (d) 0.25 and its magnified image as inset and (e) 0.48 and its magnified image as inset. 84

Figure 4.10 Scanning electron micrographs of impact fractured samples of PLA/SEBS-g-MA blends at varying Φ_d : (a) 0, (b) 0.07, (c) 0.13, (d) 0.25 and (e) 0.48. 85

Figure 4.11 Scanning electron micrographs of tensile fractured samples of PLA and PLA/SEBS-g-MA blends at varying Φ_d : (a) 0, (b) 0.07, (c) 0.13, (d) 0.25 and (e) 0.48. 87

Figure 4.12 WAXD scans of PLA, SEBS-g-MA and PLA/SEBS-g-MA blends. 88

Figure 4.13 The complex viscosity vs. angular frequency curve of PLA, SEBS-g-MA and PLA/SEBS-g-MA blends. 89

Figure 4.14 Modulus vs. angular frequency curves of PLA, SEBS-g-MA and PLA/SEBS-g-MA blends (a) storage modulus and (b) loss modulus. 90

Figure 4.15 G' and G'' vs. frequency plots of (a) PLA, (b) PLSE10, (c) PLSE20, (d) PLSE30, (e) PLSE40 and (f) SEBS-g-MA. 91

Figure 4.16 The damping factor as a function of frequency graphs for PLA, SEBS-g-MA and PLA/SEBS-g-MA blends. 92

Figure 4.17	The van Gurp-Palmen plots for PLA, SEBS-g-MA and PLA/SEBS-g-MA blends.	93
Figure 4.18	The modified Cole-Cole plots for PLA, SEBS-g-MA and PLA/SEBS-g-MA blends.	94
Figure 4.19	Variation of melt viscosity with respect to shear rate for PLA, SEBS-g-MA and PLA/SEBS-g-MA blends.	96
Figure 4.20	Load-displacement curves for PLA and PLA/SEBS-g-MA blends.	97
Figure 4.21	Hill's analysis curves for PLA and PLA/SEBS-g-MA blends.	99
Figure 4.22	Plots of (a) Specific work of fracture vs. ligament length and (b) essential work of fracture and non-essential work of fracture vs. compositions for PLA and PLA/SEBS-g-MA blends.	99
Figure 4.23	SEM micrographs of post yield fracture surfaces of PLA and PLA/SEBS-g-MA blends (a) PLA, (b) PLSE10, (c) PLSE20 and (d) PLSE40.	101

Chapter 5

Figure 5.1	DSC thermograms of PLA/SEBS-g-MA (90/10) blend and its nanocomposites at 2.5°C/min.	108
Figure 5.2	TGA curves for sepiolite, PLA/SEBS-g-MA blend and its nanocomposites. Inset: TGA of sepiolite showing four distinct weight losses.	110
Figure 5.3	d-TGA curves for PLA/SEBS-g-MA blend and its nanocomposites. Inset: d-TGA curve for sepiolite.	111
Figure 5.4	Stress-strain curves of PLA/SEBS-g-MA blend and its nanocomposites.	112
Figure 5.5	Mechanical properties of PLA/SEBS-g-MA blend and its nanocomposites (a) tensile strength (b) tensile modulus (c) elongation-at-break (d) impact strength.	113
Figure 5.6	Storage modulus vs. temperature curves of PLA/SEBS-g-MA blend and its nanocomposites.	116
Figure 5.7	Tan δ vs. temperature curves of PLA/SEBS-g-MA blend and its nanocomposites.	118
Figure 5.8	WAXD patterns of sepiolite, PLA/SEBS-g-MA blend and its nanocomposites.	120
Figure 5.9	FESEM images of sepiolite and PLA/SEBS-g-MA/sepiolite nanocomposites (a) sepiolite (b) PLSE10 (c) PLSN0.5 (d) PLSN2.5 (e) PLSN5 and (f) PLSN10.	121

Figure 5.10	FESEM images of impact fractured samples of PLA/SEBS-g-MA blend matrix and PLA/SEBS-g-MA/sepiolite nanocomposites (a) PLSE10 (b) PLSN0.5 (c) PLSN2.5 (d) PLSN5 and (e) PLSN10.	122
Figure 5.11	SEM images of tensile fractured samples of PLA/SEBS-g-MA blend matrix and PLA/SEBS-g-MA/sepiolite nanocomposites (a) PLSE10 (b) PLSN0.5 (c) PLSN2.5 (d) PLSN5 and (e) PLSN10.	123
Figure 5.12	TEM micrographs of sepiolite and PLA/SEBS-g-MA/sepiolite nanocomposites: (a) sepiolite, (b) PLSN0.5, (c) PLSN2.5, (d) PLSN5 and (e) PLSN10.	124
Figure 5.13	Modulus vs. strain (%) curves for PLA/SEBS-g-MA blend matrix and PLA/SEBS-g-MA/sepiolite nanocomposites (a) storage modulus and (b) loss modulus.	126
Figure 5.14	The complex viscosity vs. angular frequency curves for PLA/SEBS-g-MA blend matrix and PLA/SEBS-g-MA/sepiolite nanocomposites.	127
Figure 5.15	Elastic moduli vs. angular frequency curves for PLA/SEBS-g-MA blend matrix and PLA/SEBS-g-MA/sepiolite nanocomposites.	128
Figure 5.16	Viscous moduli vs. angular frequency curves for PLA/SEBS-g-MA blend matrix and PLA/SEBS-g-MA/sepiolite nanocomposites.	129
Figure 5.17	The modified Cole-Cole plots for PLA/SEBS-g-MA blend matrix and PLA/SEBS-g-MA/sepiolite nanocomposites.	131

Chapter 6

Figure 6.1	DSC second heating curves of PLA and PLA/PEG blends at 10°C/min.	136
Figure 6.2	DSC cooling curves of PLA and PLA/PEG blends at 10°C/min.	136
Figure 6.3	Storage modulus curves of PLA and PLA/PEG blends.	138
Figure 6.4	Loss modulus curves of PLA and PLA/PEG blends.	140
Figure 6.5	Tan delta curves of PLA and PLA/PEG blends. Inset: Tan delta curves of PLA and PLA/PEG blends at low temperature.	140
Figure 6.6	TGA curves for PLA, PEG and PLA/PEG blends.	142
Figure 6.7	d-TGA curves for PLA, PEG and PLA/PEG blends.	142
Figure 6.8	Flexural strength curves for PLA and PLA/PEG blends.	144
Figure 6.9	Flexural modulus curves for PLA and PLA/PEG blends.	144
Figure 6.10	Cryofractured surface morphology of PLA and PLA/PEG blends. (a) PLA, (b) PLP 10, (c) PLP20 and (d) PLP30.	145
Figure 6.11	WAXD curves for PLA, PEG and PLA/PEG blends.	146

Figure 6.12 Shear viscosity vs. shear rate plots for PLA and PLA/PEG blends.

147

List of tables

Table no.	Table Caption	Page no.
Chapter 2		
Table 2.1	Formulations for compounding in twin screw extruder for PLA/PEG blends	47
Table 2.2	Temperature profile in twin screw extruder for PLA/PEG blends.	47
Table 2.3	Temperature Profile for injection moulding of PLA/PEG blends.	47
Table 2.4	Parameters for injection moulding of PLA/PEG blends.	47
Table 2.5	Compositions and sample designations of PLA/SEBS-g-MA blends.	48
Table 2.6	Sample designations and compositions of the nanocomposites.	49
Chapter 3		
Table 3.1	Tensile properties of PLA and PLA/PEG blends.	59
Table 3.2	Tensile properties of PLA and PLA/SEBS-g-MA blends.	64
Chapter 4		
Table 4.1	Compositions, storage modulus, T_g and $\tan \delta$ value of PLA, SEBS-g-MA and PLA/SEBS-g-MA blends.	73
Table 4.2	DSC crystallization parameters for PLA in PLA/SEBS-g-MA blends.	75
Table 4.3	Thermal degradation behaviour of PLA, SEBS-g-MA and PLA/SEBS-g-MA blends.	77
Table 4.4	Values of the stress concentration factor α , Eq. (4.2), adhesion parameter K, Eq. (4.1), flexibility parameter L, Eq. (4.5), domain size (d_w) and interparticle distance (τ) in PLA/SEBS-g-MA blends.	80
Table 4.5	Compositions and designations of samples with A, B, n and K values for PLA, SEBS-g-MA and PLA/SEBS-g-MA blends.	94
Chapter 5		
Table 5.1	Summary of second heating DSC results for PLA/SEBS-g-MA blend matrix and its sepiolite based nanocomposites.	109
Table 5.2	Thermal degradation behaviour of PLA/SEBS-g-MA blend and its sepiolite based nanocomposites.	111
Table 5.3	Mechanical properties of PLA/SEBS-g-MA blend and its sepiolite based nanocomposites.	114

Table 5.4 Storage modulus, T_g and $\tan \delta$ of PLA/SEBS-g-MA blend and its sepiolite based nanocomposites. 118

Table 5.5 Designations of samples with A and B values for PLA/SEBS-g-MA blend matrix and PLA/SEBS-g-MA/sepiolite nanocomposites. 130

Chapter 6

Table 6.1 DSC crystallization parameters (second heating and cooling) for PLA, PEG and PLA/SEBS-g-MA blends. 137

Table 6.2 Storage modulus, T_g and $\tan \delta$ values for PLA and PLA/PEG blends. 139

Table 6.3 Thermal degradation data for PLA, PEG and PLA/PEG blends. 143

Table 6.4 Designations of samples with n and K values for PLA and PLA/PEG blends. 148

List of abbreviations & symbols

ASTM	American Society for Testing Materials
CSM	Chlorosulfonated polyethylene rubber
CTOD	Crack tip opening displacement
DMA	Dynamic mechanical analysis
DSC	Differential scanning calorimetry
d-TGA	First derivative thermogravimetric analysis
D _w	Weight average particle diameter
EWf	Essential work of fracture
FESEM	Field emission scanning electron microscopy
HDPE	High density polyethylene
IFPZ	Inner fracture process zone
MFI	Melt flow index
MMT	Montmorillonite
OPDZ	Outer plastic deformation zone
PA	Polyamide
PC	Polycarbonate
PLA	Poly lactide/ poly(lactic acid)
POM	Poly(oxy methylene)
PP	Polypropylene
PS	Polystyrene
iPP	Isotactic polypropylene
SBS	Styrene-butadiene-styrene block copolymer
SEBS	Styrene-(ethylene-butylene)-styrene block copolymer
SEBS-g-MA	Maleic anhydride grafted styrene-(ethylene-butylene)-styrene

TEM	Transmission electron microscopy
TGA	Thermogravimetric analysis
T_{cc}	Cold crystallization temperature
T_f	Final decomposition temperature
T_g	Glass transition temperature
T_m	Melting temperature
T_{max}	Temperature at maximum rate of weight loss
T_{onset}	Onset degradation temperature at 5% weight loss
WAXD	Wide-angle X-ray diffraction
X_m	Degree of melt crystallinity
X_{cc}	Degree of crystallinity because of cold crystallization
ΔH_m	Heat of melting
α	Stress concentration factor
β	Plastic shape factor
δ	Phase angle
Φ_d	Volume fraction of SEBS-g-MA
E_b	Tensile modulus of blends
E_d	Tensile modulus of the disperse phase i.e. SEBS-g-MA
E_p	Tensile modulus of PLA
E	Tensile modulus
E'	Storage modulus
E''	Loss modulus
ε_b	Elongation-at-break of the blends
ε_p	Elongation-at-break of PLA
G^*	Complex modulus

G'	Elastic modulus
G''	Viscous modulus
K	Phase interaction constant
L	Flexibility coefficient
σ_b	Tensile strength of blends
σ_p	Tensile strength of PLA
τ	Matrix ligament thickness
η^*	Complex viscosity
W_e	Essential work of fracture
W_p	Non-essential work of fracture